

## [12] Characterization of R9AP, a Membrane Anchor for the Photoreceptor GTPase-Accelerating Protein, RGS9-1

By GUANG HU and THEODORE G. WENSEL

### Abstract

The proper recovery of photoreceptor light responses requires timely inactivation of the G-protein transducin ( $G_t$ ) by GTP hydrolysis. It is now well established that the GTPase-accelerating protein (GAP) RGS9-1 plays an important role in determining the recovery kinetics of photoreponses. RGS9-1 has been found to be anchored to photoreceptor disk membranes by a novel photoreceptor protein, R9AP. R9AP has a single transmembrane domain at its C-terminal region. Membrane tethering by R9AP enhances RGS9-1 GAP activity *in vitro* and has been hypothesized to be important for the regulation of RGS9-1 function *in vivo*. In addition, R9AP shows structural similarity to the SNARE complex protein syntaxin and has been shown to be required for the correct targeting and localization of the RGS9-1 protein in photoreceptors. Therefore, R9AP may have additional functions other than that in the phototransduction pathway.

This article presents methods and protocols developed for the functional characterization of R9AP in phototransduction, including the immunoprecipitation of the endogenous protein, the expression and purification of recombinant proteins, the reconstitution of proteoliposomes, and assays for its interaction with RGS9-1 and its effects on RGS9-1 GAP activity. These methods may also be applied to the study of R9AP function in other pathways or other cell types or to the studies of other membrane proteins that are structurally similar to R9AP.

### Introduction

In phototransduction, deactivation in a timely fashion of the G-protein  $\alpha$  subunit, transducin- $\alpha$  ( $G_{t\alpha}$ ), by GTP hydrolysis is important in the regulation of light responses in vertebrate photoreceptors (Lyubarsky and Pugh, 1996; Pugh, 2000; Sagoo and Lagnado, 1997). A member of the RGS protein family, RGS9-1 accelerates GTP hydrolysis on  $G_{t\alpha}$  and plays a central role in determining the inactivation kinetics of phototransduction (Chen *et al.*, 2000; He *et al.*, 1998; Lyubarsky *et al.*, 2001; Makino *et al.*, 1999; Zhang *et al.*, 2003). RGS9-1 is the endogenous GTPase-accelerating protein (GAP) for  $G_{t\alpha}$  and is the mammalian RGS protein

whose physiological function has been characterized most thoroughly (reviewed in Cowan *et al.*, 2001). It is a peripheral membrane protein on the photoreceptor outer segment membranes (Cowan *et al.*, 1998) and is tethered to the membranes by a newly identified retinal protein, R9AP (Hu and Wensel, 2002). R9AP was discovered by its interaction with RGS9-1 in detergent extracts from rod outer segment membranes (ROS) and was found to bind directly to the N-terminal region of RGS9-1. It is expressed predominantly in the retina and localizes largely in the photoreceptor outer segment layer. It has a single transmembrane helix in its C-terminal region and serves as a membrane anchor for RGS9-1 (Hu and Wensel, 2002).

Studies have shown that membrane anchoring of RGS9-1 by R9AP enhances its GAP activity toward  $G_{\text{ta}}$  *in vitro* (Hu *et al.*, 2003), and this membrane anchoring can be regulated by the phosphorylation state of RGS9-1 (Sokal *et al.*, 2002). Therefore, R9AP may play a role in the modulation of phototransduction recovery kinetics. In addition, R9AP also seems to play a role in the sorting of RGS9-1 protein in photoreceptors. Expression of a mutant RGS9-1 that has impaired interaction with R9AP but intact GAP activity resulted in mislocalization of the mutant protein and complete loss of GTPase acceleration in phototransduction in mice.

R9AP orthologs have been identified in human, cattle, mouse, rat, *Xenopus*, zebrafish, and puffer fish (Hu and Wensel, 2002; Hu *et al.*, 2003). Expressed sequence tags of R9AP have been found in cDNA from human fetal eye (BQ187216), human kidney (AW302149), adult mouse retina (BB591662, BI730314), pig (BX665878, BX667653), *Xenopus laevis* brain (CD328477, CD328533, CD303540, CD256685), whole 31–32 stage embryo (CF288302) and lung (BG515592), *Xenopus (Silurana) tropicalis* (BX667653), zebrafish adult retina (BE015922), and three-spined stickleback fish (CD507448).

Although there are two distinct R9AP-like sequences among *Xenopus* expressed sequence tags (ESTs), there is only one intronless R9AP gene and no close homolog in available human and mouse genome sequences. There are many distant homologs, as the structure of R9AP predicted by computational methods is similar to the syntaxin family of SNARE proteins involved in vesicle trafficking.

This article describes the experimental procedures developed to characterize the function of R9AP in phototransduction, including protocols for isolation of the endogenous protein from retinal extract, expression and purification of recombinant proteins, reconstitution of proteoliposomes, and assays for its interaction with RGS9-1 and its effect on RGS9-1 GAP activity. An interesting feature of R9AP is that it is one of a very few mammalian transmembrane proteins that can be expressed in *Escherichia coli*, purified in detergent, and reconstituted in active form in lipid vesicles. It

is hoped that these methods will not only be helpful in further investigations of the function of R9AP in photoreceptors, but in future studies on its potential functions in other organs or cell types as well.

### Immunoprecipitation of RGS9-1 and R9AP from ROS Extract

To understand how the function of RGS9-1 is regulated, it is useful to know the proteins with which it interacts. We took a proteomics approach and developed an affinity purification protocol to isolate the RGS9-1 complex efficiently from rod outer segment membranes. The protocol allowed us to extract the majority of the ROS membrane proteins into solution, including the major signaling components in phototransduction, and to obtain a sufficiently large quantity of pure RGS9-1 or R9AP protein complex for sequence analysis and further study.

### *Buffers and Reagents*

GAPN buffer: 100 mM NaCl, 10 mM HEPES, pH 7.4, 2 mM MgCl<sub>2</sub>, 1 mM dithiothreitol (DTT), solid phenylmethylsulfonyl fluoride (PMSF), ~20 mg/liter). In this and other buffers, PMSF crystals are added at an amount above its solubility in water and maintained in suspension as a continuous source of PMSF, which is poorly soluble and fairly rapidly hydrolyzed once in solution. The buffers are filtered routinely through nitrocellulose filters with 0.2- or 0.45- $\mu$ m pores before use, and the PMSF is added after filtration

Solubilization buffer: 1% NP40 (Sigma) in GAPN, without DTT *n*-Octyl- $\beta$ -D-glucopyranoside (Anatrace)

Antibodies: Rabbit anti-RGS9-1c polyclonal antiserum, anti-RGS9-N polyclonal antiserum, monoclonal anti-RGS9-1 antibody D7, and polyclonal goat anti-R9AP antiserum (Cowan *et al.*, 1998; He *et al.*, 1998, 2000; Hu and Wensel, 2002)

CNBr-activated Sepharose 4B (Amersham Biosciences)

Protein A-Sepharose 4 fast flow (Amersham Biosciences)

*Procedures.* ROS are isolated from frozen bovine retina by a standard procedure (Papermaster and Dreyer, 1974; Papermaster, 1982) and stored at  $-80^{\circ}$ . Purified ROS are pelleted by centrifugation at 84,000g at  $4^{\circ}$  and washed with GAPN buffer using the same centrifugation conditions and a rhodopsin concentration of 10–15  $\mu$ M. The membranes are then dissolved in detergent at a rhodopsin concentration of 60  $\mu$ M by homogenization in syringes with 18- or 23-gauge needles and incubation at  $0-4^{\circ}$  for 30 min with gentle agitation to solubilize ROS membrane proteins. Both 40 mM

octyl-glucoside and 1% NP40 in GAPN are found to solubilize RGS9-1 efficiently, and NP40 is chosen in routine preparations due to its lower cost. Insoluble proteins (the major one is tubulin) are removed by centrifugation at 84,000g, and the supernatant (containing the majority of ROS proteins) is collected for immunoprecipitation.

To prepare antibody-coupled Sepharose beads for immunoprecipitation, IgG is first purified from rabbit anti-RGS9-1c antiserum using protein A—Sepharose 4 fast flow affinity chromatography (Harlow and Lane, 1988), or from goat anti-R9AP antiserum following a protocol of Gray *et al.* (1969) and Ibrahimi *et al.* (1980). Purified IgG is then coupled to CNBr-activated Sepharose 4B at a ratio of 10 mg IgG to 1 ml beads according to the manufacturer's instructions (Amersham Biosciences). IgG that is not coupled covalently to the beads is removed by washing the beads alternately using 0.1 M Tris-HCl, pH 8.0, 0.5 M NaCl, and 0.1 M CH<sub>3</sub>COONa, pH 4.0, 0.5 M NaCl for four to five times. Beads are stored in 0.1 M Tris-HCl, pH 8.0, 0.5 M NaCl at 4° as ~50% slurry and can be stored for up to 1 year (sodium azide can be added to prevent contamination by microorganisms, but is not necessary) without a significant decrease in its efficiency in immunoprecipitation. However, some detachment of IgG from the beads is observed after long-term storage. Before every immunoprecipitation experiment, antibody-coupled beads need to be washed again more stringently with 0.1 M glycine, pH 2.5, two to three times and then equilibrated in ROS solubilization buffer. This step removes loosely attached IgG light chains or any residual detached IgGs from the beads and therefore is critical in reducing IgG contamination in the final immunoprecipitation product. IgG light chains and heavy chains appear on SDS-PAGE as diffuse bands at apparent sizes of ~25 and ~55 kDa, respectively, and interfere with R9AP and RGS9-1 detection on Coomassie-stained gels.

Small-scale RGS9-1 immunoprecipitation from detergent-solubilized ROS membranes is performed by incubating 300  $\mu$ l solubilized ROS with 40  $\mu$ l IgG-coupled beads for 2.5 h at 4° with mixing on a shaker. Beads are then separated from the supernatant by a brief centrifugation and are washed three times with the solubilization buffer. Bound proteins are eluted from the beads by 0.1 M glycine at pH 3.0, concentrated by trichloroacetic acid precipitation, and redissolved in the SDS-PAGE sample buffer. Under these conditions, more than 90% of the RGS9-1 (~0.5–1  $\mu$ g) in the ROS can be immunoprecipitated and recovered in the eluted proteins. To measure the efficiency of immunoprecipitation, eluted proteins are resolved by SDS-PAGE, and RGS9-1 is detected by immunoblotting using the monoclonal antibody D7. Under these conditions, ~90% or more of the RGS9-1 protein can be depleted from the retinal extract and eluted

from the beads (see [Hu \*et al.\*, 2001](#)). For large-scale immunoprecipitation of RGS9-1, 2 ml of anti-RGS9-1c IgG-coupled Sepharose beads is packed into a column, and detergent extracts of ROS membranes (equivalent to 50–100 mg rhodopsin) are incubated with the beads in the column with shaking at 4° for 3–4 h. The column is washed with 40–60 ml solubilization buffer, and proteins are eluted stepwise with 0.1 M glycine, pH 3.0, at 1 ml per sample for a total of 20 ml. Eluted proteins are precipitated by 10% trichloroacetic acid (TCA), washed with acetone, resuspended in SDS-PAGE sample buffer, resolved by SDS-PAGE, and visualized by Coomassie staining. Milligrams of the RGS9-1 complex can be isolated using this method in a heterotetrameric complex with  $G_{\beta 5L}$ ,  $G_{t\alpha}$ , and R9AP with minimal residual contamination from other retinal proteins. The stoichiometry of the proteins in the complex is in an approximate molar ratio of 1:1:1:1 ([Hu and Wensel, 2002](#)) ([Fig. 1](#)), although the relative amount of  $G_{t\alpha}$  is somewhat variable.

Similar procedures are used for the immunoprecipitation of R9AP. However, because R9AP is a membrane protein and precipitates in buffers without detergent, the SDS-PAGE sample buffer is used to elute it from the antibody-coupled beads. The concentration of the reducing reagents in the sample buffer has to be minimized and elution has to be done at room temperature in 2–5 min in order to reduce the elution of IgG light chains from the beads.

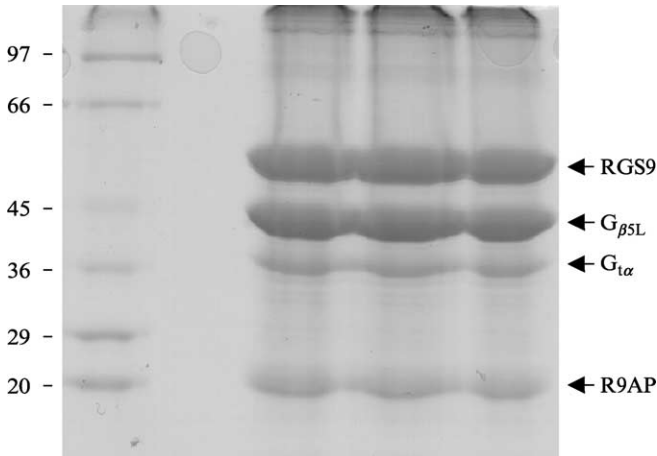


FIG. 1. Preparative immunoprecipitation for R9AP sequence analysis. Detergent-solubilized ROS proteins were immunoprecipitated as described in the text, separated on a preparative SDS-PAGE, and stained with Coomassie blue dye.

## Localization of R9AP in the Retina

### *Immunofluorescence Microscopy*

#### *Buffers and Reagents*

PBST: 155 mM NaCl, 1.5 mM  $\text{KH}_2\text{PO}_4$ , 2.7 mM  $\text{Na}_2\text{HPO}_4$ , pH 7.2, 0.1% Triton X-100

Antibodies: polyclonal goat anti-R9AP antiserum, Texas Red-labeled rabbit antigoat antibody (Vector Laboratories)

Sheep serum (Sigma)

Vectashield mounting solution (Vector Laboratories)

C57BL-6 mice

*Procedures.* Mouse eyes are dissected, fixed, cryoprotected with sucrose buffer, frozen, and then cryosectioned (Lyubarsky *et al.*, 2001). Sections are blocked with 10% sheep serum (Sigma) in PBST for 1 h and are then incubated with goat anti-R9AP antiserum at a 1:500 dilution in PBST for 2 h. For control experiments, the 1:500 diluted goat anti-R9AP antiserum is neutralized with 0.1 mg/ml recombinant His-R9AP- $\Delta\text{C}$  (see later for preparation) in PBST before being applied to the sections. After a 2-h incubation, sections are washed three times for 5 min in PBST to remove excess antibodies, and the Texas Red-labeled rabbit antigoat antibody is added to the sections at a dilution ratio of 1:100 and incubated for 1 h. The sections are washed again in PBST three times for 5 min, mounted using Vectashield mounting solution, and imaged using an LSM-510 confocal microscope (Zeiss). R9AP staining is largely detected in the photoreceptor outer segments, with stronger signals in the cones than rods. Staining in the inner segments is also detectable, but with less intensity. Note that the strong labeling of the outer plexiform layer is very likely caused by the cross-reactivity of the antibody toward syntaxin-like proteins, which share structural similarity to R9AP and are highly concentrated in the synaptic junctions between photoreceptors and bipolar cells (see later for more supporting evidence) (Hu and Wensel, 2002).

### *Localization by Fractionation of Retinal Membranes*

The R9AP signal is largely detected in the photoreceptor layer of the retina and is enriched in the photoreceptor outer segments by immunofluorescence, suggesting its function in phototransduction. However, strong labeling is also observed at the outer plexiform layer where RGS9-1 labeling is not obvious. Therefore, to find out if there is a distinct population of R9AP that is not associated with RGS9-1, we also use biochemical methods to investigate its localization and interaction with RGS9-1 in the retina.

### Reagents

**Antibodies:** polyclonal goat anti-R9AP antiserum, polyclonal anti-RGS9-1c antiserum

**Procedures.** Because RGS9-1 is only observed in the photoreceptor outer segment in immunofluorescence studies, we separate retinal membranes into ROS membranes and ROS-depleted membranes and test whether there is R9AP present in ROS-depleted membranes and whether it exists in the RGS9-1-free form. Forty bovine retinas are extracted twice with 20 ml 34% sucrose buffer by gentle vortexing. The resulting crude ROS and ROS-depleted retinal membranes are separated by a 20-min low-speed centrifugation at 6000 rpm in a Beckman JA 25.50 rotor. The supernatants are pooled, diluted four to five times in GAPN, and centrifuged at 15,000 rpm in the same rotor to collect ROS membranes. The ROS or ROS-depleted membranes are solubilized in 1% NP40 in GAPN, and RGS9-1 is immunodepleted from the detergent-solubilized proteins as described in the previous section. R9AP in the samples before and after RGS9-1 depletion is determined by immunoblotting. In both ROS or ROS-depleted fractions, complete RGS9-1 depletion results in 100% R9AP depletion, indicating that all the R9AP protein must be in complex with RGS9-1 in the retina (Hu and Wensel, 2002).

To test whether R9AP localizes predominantly to fractionated ROS membranes, ROS membranes from frozen bovine retinas are prepared in dim red light and separated by sucrose gradient centrifugation using a standard technique (Papermaster and Dreyer, 1974). Samples in the sucrose gradient are fractionated into 1-ml aliquots using an automatic gradient puller (Auto-Densi-Flow from Labconco) and stored at  $-80^{\circ}$ . Proteins in these fractions are resolved by SDS-PAGE, and R9AP is detected by Western blotting. The concentration of the major rod outer segment marker protein rhodopsin in these fractions is determined by measuring the difference of absorbance at 500 nm before and after light bleaching in 1.5% *N,N*-dimethyldodecylamine *N*-oxide. We observed faithful copurification of R9AP and rhodopsin, strongly supporting the conclusion that R9AP is localized within ROS membranes (Hu and Wensel, 2002).

### Expression and Purification of Recombinant R9AP

To characterize the biochemical properties of R9AP, it is necessary to generate recombinant proteins for *in vitro* functional assays and antibody production. Although *E. coli* has been the most commonly used

heterologous expression system, there are few examples of purification and reconstitution of functional mammalian transmembrane proteins from bacteria (Quick and Wright, 2002). We have developed a successful strategy for preparation of R9AP in *E. coli*, and this strategy may also be applicable to other membrane proteins of similar type. We also developed a protocol to express R9AP in insect cells. These highly efficient expression and purification methods may facilitate future structural studies of the GAP complex.

### *Buffers and Reagents*

Lysis buffer: 300 mM NaCl, 25 mM Tris, pH 8.0, 20 mM imidazole, 2 mM DTT and solid PMSF (~20 mg/liter)

Dialysis buffer: 10 mM Tris-HCl, 1 mM DTT, pH 8.0

Sodium cholate (3 $\alpha$ , 7 $\alpha$ , 12 $\alpha$ -trihydroxy-5 $\beta$ -cholic acid sodium salt), Sigma

Isopropyl- $\beta$ -D-thiogalactopyranoside (IPTG)

Plasmids: pET14b (Novagen) and pVL1392 (BD Biosciences).

*E. coli* strain BL21 (DE3) LysS (Novagen)

BD BaculoGold baculovirus expression vector system (BD Biosciences)

Sf9 cells (serum-free medium adapted) (Invitrogen)

SF900 II serum-free insect cell medium (Invitrogen)

Ni-NTA superflow beads (Qiagen)

POROS HQ strong anion-exchange column (Applied Biosystems)

*Procedures.* Bovine R9AP fragment (His-R9AP- $\Delta$ C, amino acid 1–212), or His-R9AP- $\Delta$ C2, amino acid 1–191) and mouse R9AP full-length cDNA (His-mR9AP) are amplified by polymerase chain reaction from bovine retina cDNA library and mouse genomic DNA, respectively, and cloned into the pET14b vector using *Bam*HI and *Nde*I sites (Hu and Wensel, 2002). N-terminal His<sub>6</sub>-tagged bovine R9AP domains or mouse full-length R9AP protein is expressed in *E. coli* [BL21(DE3) LysS] by growing freshly transformed cells to OD<sub>600</sub> ~0.6–0.8 and inducing with 0.3 mM IPTG at 30° for 4–5 h. Cells are harvested by centrifugation at 3000g and can be stored at –80° until use. Under these conditions, ~10 mg protein can be produced in every liter of culture. Bovine R9AP fragments are largely soluble, as they do not contain the C-terminal transmembrane helix, and the mouse full-length protein is insoluble.

For insect cell expression, the N-terminal His<sub>6</sub>-tagged mouse full-length R9AP was cut out of pET14b using *Xba*I and *Nde*I sites and cloned into pVL1392. The resulting plasmid is used to generate baculoviruses that can

infect and express R9AP in insect cells using the BaculoGold system (BD biosciences). *Sf9* cells are seeded at  $1.0 \times 10^6$  cells/ml in serum-free SF900 II medium and are infected with the R9AP viruses at MOI (multiplicity of infection) of 3 after 24 h of growth at 28°. Cells are grown for another 50–54 h postinfection and are then harvested by centrifugation. About 0.5 mg protein can be obtained from every liter of culture.

Because *E. coli* expression is much more economical and time-saving, it is used routinely to obtain large quantities of recombinant R9AP. To purify His-R9AP- $\Delta$ C or His-R9AP- $\Delta$ C2, *E. coli* cells are resuspended in lysis buffer and lysed by sonication. Cell debris and insoluble materials are removed by centrifugation at 24,000g in a Beckman JA 25.50 rotor for 30 min. R9AP-soluble fragments in the supernatant are purified by affinity chromatography using nickel nitrilotriacetate (Ni-NTA superflow beads, Qiagen) according to the manufacturer's protocol. Proteins are eluted with 200 mM imidazole in the lysis buffer, and the purest fractions are combined and dialyzed against dialysis buffer. After dialysis, proteins are loaded onto a POROS HQ anion-exchange HPLC column (Applied Biosystems), washed with 20 mM NaCl in dialysis buffer, and eluted with a linear gradient from 20 to 200 mM NaCl in the same buffer. The flow rate is kept at 2 or 3 ml/min because a faster flow rate decreases resolution. The purest fractions are combined, concentrated to  $\sim$ 2–4 mg/ml, and stored at 4° for short-term usage or at  $-20^\circ$  after adding glycerol to 40% for long-term usage (Hu and Wensel, 2002).

To purify His-mR9AP, *E. coli* cells are lysed, and insoluble proteins including R9AP are separated from soluble proteins in a similar way. The insoluble proteins, including His-mR9AP, are washed once in lysis buffer and are then extracted with 4% sodium cholate in lysis buffer for  $\sim$ 30–60 min at 4° with gentle agitation, and the detergent-solubilized proteins in the supernatant are separated from the pellet by centrifugation. The extraction is repeated a total of three to four times, yielding  $>70\%$  of total His-mR9AP extracted in soluble form (Hu *et al.*, 2003). Being in the insoluble fraction actually facilitates purification, as most contaminating *E. coli* proteins are soluble and are removed in the beginning. The detergent supernatants are pooled together and applied to Ni-NTA beads, and His-mR9AP is purified in 4% sodium cholate in lysis buffer according to the manufacturer's protocol. From 2 liters of *E. coli* culture, at least 5 mg R9AP with 90–95% purity can be obtained routinely. It should be noted that discarding the supernatant from the first detergent extraction can improve the purity of the final product, although at the expense of lowering the yield, as the first extract contains some *E. coli* proteins that copurify with R9AP on Ni-NTA beads.

## Vesicle Reconstitution

Because R9AP is a transmembrane protein, it is necessary to reconstitute it into lipid vesicles to study its function in its natural conformation. The protocol we developed to reconstitute R9AP and rhodopsin into lipid vesicles allowed us to reconstitute much of the vertebrate visual cascade *in vitro*. It will facilitate further studies on the effect of specific lipids and other molecules of ROS membranes in regulating RGS9-1 activity. It may also be useful in the characterization of other phototransduction components or be applied to the studies of membrane proteins of similar types in other systems.

## Reagents

L- $\alpha$ -Phosphatidylserine (PS: brain, porcine-sodium salt) (Avanti Polar Lipids)

L- $\alpha$ -Phosphatidylcholine (PC: egg, chicken) (Avanti Polar Lipids)

L- $\alpha$ -Phosphatidylethanolamine (PE: egg, chicken) (Avanti Polar Lipids)

Rhodamine-labeled PE [*N*-(6-tetramethylrhodaminethiocarbamoyl)-1,2-dihexadecanoyl-*sn*-glycero-3-phosphoethanolamine, triethylammonium salt] (Molecular Probes Inc.)

Sodium cholate (Sigma)

*Procedures.* Lipids are mixed at a ratio (w/w) of PC:PE:PS = 50:35:15 to mimic the ROS phospholipid composition (Daemen, 1973). They are mixed in chloroform, dried under argon flow, and redissolved in 4% sodium cholate in lysis buffer to a final concentration of 20 mg/ml. To facilitate the use of vesicles in binding assays, those used for this purpose contain rhodamine-labeled PE at a final concentration of 0.5% (w/w) to help in visualizing the lipids. Lipids in detergent solution are mixed with purified rhodopsin, His-mR9AP, or rhodopsin plus His-mR9AP, each in the same detergent concentration, using a lipid to protein (w/w) ratio of 20–40:1. The mixture is dialyzed against GAPN buffer ( $>100 \times$  volume) with buffer changes every 20–24 h for a total of approximately 120 h (Parmar *et al.*, 1999). Dialyzed samples are centrifuged (15 min, 18,000g, Beckman TL100 rotor) to remove any aggregates. Reconstituted proteoliposomes are in the supernatant at this point in the procedure and contain the majority of the protein added initially to the reaction mixture in a roughly random orientation with respect to the inner and outer membrane leaflets. The resulting proteoliposomes are unilamellar and have a fairly narrow size distribution: radius = 240 ( $\pm$  50) Å (Fig. 2).

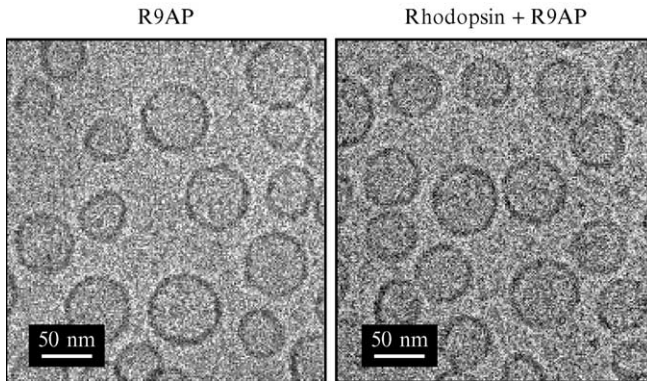


FIG. 2. Electron micrographs of reconstituted vesicles, imaged in vitreous ice. The reconstituted vesicles (in solution) were frozen on carbon-coated holey grids by rapid plunging into liquid ethane. Images were recorded at a nominal magnification of  $40,000\times$  with a dose of  $\sim 20$  electrons per  $\text{\AA}^2$  on a JEOL1200EX electron microscope. R9AP, R9AP-only vesicles; rhodopsin + R9AP, rhodopsin and R9AP vesicles. Reprinted, with permission, from Hu *et al.* (2003).

Two different methods are used to concentrate the vesicles. R9AP-only vesicles are concentrated by ultracentrifugation at  $88,000g$ . The easily pelleted vesicles are collected to be used in binding assays, and vesicles that stay in the supernatant are discarded. Pelleted vesicles are resuspended in GAPN buffer to the desired concentration by repeated extrusion through a 26-gauge needle. Lipid-only vesicles used as controls in the binding assays are made similarly in parallel, except that the proteins are left out. However, lipid-only vesicles are less dense than R9AP vesicles and do not pellet as well. Therefore, disturbance of the pellet should be minimized to avoid mixing the pellet with the supernatant. Rhodopsin or rhodopsin and R9AP vesicles (Fig. 2), which do not pellet as efficiently as the R9AP-only vesicles, are concentrated in a protein concentrator (50 kDa cutoff, Millipore) by centrifugation to collect all the vesicles and obtain the maximum yield. Concentrated samples are then diluted to the desired concentrations in GAPN buffer.

Lipid concentrations of all the samples are determined by measuring the total phosphate concentrations colorimetrically (Chen *et al.*, 1956). The concentrations of vesicles expressed in terms of “moles” are calculated as follows: molar concentration of vesicles = (formal concentration of phospholipids  $\times s$ )/ $4\pi r^2$ , where  $s$  is the average surface area of a phospholipid head group in  $\text{\AA}^2$  ( $70 \text{\AA}^2$ ) and  $r$  is the average vesicle radius in  $\text{\AA}$ . Rhodopsin concentrations are determined from bleachable absorbance at 500 nm

( $\epsilon = 40,600 \text{ M}^{-1}\text{cm}^{-1}$ ) in lauryldimethylamine oxide (1.5%, v/v). R9AP concentrations are determined by the densitometry of Coomassie-stained SDS-PAGE gels using bovine serum albumin as the standard. The molar ratios of R9AP, rhodopsin, and vesicles are fairly constant across different batches of the vesicles, as they are largely determined by the amount of R9AP, rhodopsin, and lipids used in the reconstitution.

### Binding of R9AP and RGS9-1

Because RGS9-1 forms a heterotetramer with  $G_{\beta 5L}$ ,  $G_{t\alpha}$ , and R9AP, binding assays between RGS9-1 and R9AP are carried out to test the direct interaction between RGS9-1 and R9AP and to identify the domains on RGS9-1 responsible for this interaction. Binding assays between RGS9-1 and the R9AP-soluble domain are carried out using the His<sub>6</sub>-tagged R9AP soluble domain immobilized on Ni<sup>2+</sup>-NTA beads. Binding to full-length R9AP is measured by reconstituting detergent-solubilized recombinant R9AP into vesicles and separating vesicle-bound proteins by centrifugation.

### Buffers and Reagents

Binding buffer: 100 mM NaCl, 10 mM HEPES, pH 7.4, 2 mM MgCl<sub>2</sub>, 0.5% NP40, 10 mM imidazole, and 0.5 mg/ml chicken egg ovalbumin Ni-NTA superflow beads (Qiagen)

*Procedures.* GST-RGS9-1 (amino acid 1–484)· $G_{\beta 5}$ , GST-RGS9-1-NG (amino acid 1–280), GST-RGS9-1-NGD (amino acid 1–431)· $G_{\beta 5}$ , and His-RGS9-1-IGRC (amino acid 112–484)· $G_{\beta 5}$  complexes are expressed and purified from *Sf9* cells as described previously (He *et al.*, 2000; Martemyanov and Arshavsky, 2002). GST-tagged RGS9-1-D (amino acid 276–431) is expressed and purified from *E. coli* (Slep *et al.*, 2001). The His-RGS9-1-IGRC· $G_{\beta 5}$  complex cannot be used for assays of binding to the Ni<sup>2+</sup>-NTA-immobilized R9AP soluble domain, but can be used in vesicle-binding assays.

For a typical binding reaction between the RGS9-1 and R9AP-soluble domain, 0.5  $\mu\text{M}$  of GST-RGS9-1· $G_{\beta 5}$  or another GST-tagged RGS9-1 fragment is mixed with 2.5  $\mu\text{M}$  His-R9AP- $\Delta\text{C2}$  in 200  $\mu\text{l}$  binding buffer and incubated at 4° for 1 h. The mixtures are then incubated with 20  $\mu\text{l}$  Ni-NTA superflow beads on a shaker for another 1.5 h. The presence of detergent minimizes the nonspecific binding of RGS9-1 to the beads and the microtubes. The beads are separated from the supernatant by brief centrifugation and are washed three times with the binding buffer. Bound proteins are eluted from the beads with SDS-PAGE sample buffer, and RGS9-1 proteins or  $G_{\beta 5}$  in the elution is detected by immunoblotting using anti-RGS9-N antiserum or anti- $G_{\beta 5}$  antiserum. Control experiments are

performed similarly, except that His-R9AP- $\Delta$ C2 is not added. Both full-length RGS9-1  $\cdot$  G $\beta_5$  and RGS9-1NG  $\cdot$  G $\beta_5$  are found to bind to R9AP, whereas RGS9-1G  $\cdot$  G $\beta_5$  does not, suggesting that the NG domain (which includes the DEP domain) of RGS9-1 is responsible for the interaction (Hu and Wensel, 2002).

For binding of RGS9-1 proteins to R9AP vesicles, purified GST-RGS9-1 proteins (in GAPN buffer) are first centrifuged at 88,000g for 40 min (TLA 100.3 rotor) to remove possible aggregates. Soluble proteins in the supernatant are diluted and mixed with R9AP vesicles or lipid-only vesicles in a volume of 300  $\mu$ l and are incubated at 4 $^\circ$  with very gentle vortexing for  $\sim$ 3 h in GAPN buffer containing 0.2 mg/ml ovalbumin. One hundred microliters of the reaction mixture is then transferred to a new polypropylene tube (Beckman), and unbound proteins are separated from bound proteins by ultracentrifugation at 88,000g for 40 min. The pink (due to the rhodamine tag) vesicle pellet is redissolved in SDS-PAGE sample buffer and is subjected to electrophoresis. Again, the pellet of lipid-only vesicles is not as tight as that of the R9AP vesicles and has to be handled very gently to avoid disturbance. Typical final concentrations in binding reactions are RGS9-1 proteins, 0.1–0.5  $\mu$ M; R9AP (total), 3.0  $\mu$ M; and lipids (as phosphate), 0.8 mM. For SDS-PAGE, equal proportions of each fraction, including the starting reaction mixture, should be loaded on SDS-PAGE for easy comparison. RGS9 proteins are detected by immunoblotting with anti-RGS9-1c antiserum (see Hu *et al.*, 2003). RGS9-1  $\cdot$  G $\beta_5$ , RGS9-1NGD  $\cdot$  G $\beta_5$ , and RGS9-1GDC  $\cdot$  G $\beta_5$  all bound to R9AP vesicles, with significantly less binding detected for RGS9-1GDC  $\cdot$  G $\beta_5$ . RGS9-1D did not bind at all. Again, these results indicate that the NG domain is important for the interaction, in agreement with the findings from the aforementioned binding assays using the R9AP-soluble domain (Hu *et al.*, 2003) and with work by others (Lishko *et al.*, 2002).

#### Effect of R9AP on RGS9-1 GAP Activity

Two kinetic approaches for measuring GTPase activity have been developed previously: the multiple turnover and the single turnover method (reviewed in Cowan *et al.*, 2000). The multiple turnover method monitors the steady-state GTP hydrolysis rate during cycles of GTPase activation by the receptor and inactivation by GTP hydrolysis. The use of this assay requires that GTP hydrolysis must be the rate-limiting step. However, in experiments containing the other proteins that may interfere with GTPase recycling, such as PDE $\gamma$ , this assay could yield ambiguous results. Therefore, to avoid any possible interference caused by G-protein recycling, we used single turnover G $_{\text{at}}$  GTPase assays (Cowan

*et al.*, 2000; He and Wensel, 2001) to determine the effect of R9AP on the GAP activity of RGS9-1. We first tested the effect on the reconstituted vesicles and then tested it on urea-treated ROS membranes in which the endogenous R9AP was made accessible to recombinant RGS9-1. Note that the procedures used here employ GST-tagged RGS9-1. Lower GAP activity in the absence of R9AP and higher GAP activity in its presence were measured for a His<sub>6</sub>-tagged form of the RGS9-1/Gβ5 complex (Martemyanov and Arshavsky, 2002).

### *Enhancement of RGS9-1 GAP Activity by R9AP Vesicles*

*Procedures.* Rhodopsin vesicles or rhodopsin and R9AP vesicles are mixed with purified G<sub>t</sub> [purified from bovine retina (Struthers *et al.*, 2000)], His<sub>6</sub>-tagged PDEγ [expressed and purified from *E. coli* (He *et al.*, 2000)], and individual GST-tagged RGS9-1 proteins (GST-RGS9-1-D or GST-RGS9-1-Gβ5) in GAPN buffer and incubated on ice for ~30 min to allow for the binding between RGS9-1 and R9AP. The reaction is started by the [γ-<sup>32</sup>P]GTP addition and is stopped by the addition of trichloroacetic acid (5% w/v) at different times. Released phosphate is isolated by binding to activated charcoal, and radioactivity is measured using scintillation counting (for detailed procedures, see Cowan *et al.*, 2000; He *et al.*, 2000). Basal GTP hydrolysis rates by G<sub>tα</sub> are measured similarly by leaving out the RGS9-1 proteins in the aforementioned reactions. Typical final protein concentrations in the reactions are 4.0 μM total rhodopsin, 0.5 μM G<sub>tα</sub>, 0.1 μM RGS9-1, 0.2 μM His<sub>6</sub>-PDEγ, and 1.2 μM R9AP; the final GTP concentration is 25 nM. Data are fitted to a single exponential curve to derive the GTP hydrolysis rate constant  $k_{\text{inact}}$ . RGS9-1 GAP activity ( $\Delta k_{\text{inact}}$ ) is calculated as  $\Delta k_{\text{inact}} = k_{\text{inact}}(\text{of } G_{t\alpha} \text{ in the presence of RGS9-1}) - k_{\text{inact}}(\text{of } G_{t\alpha})$ .

At a given RGS9-1 concentration, the apparent RGS9-1 GAP activity is expected to be a function of the vesicle concentration. On the one hand, an increasing vesicle concentration increases the total R9AP concentration, and therefore increases the fraction of RGS9-1 that can be anchored to the vesicles, which will eventually be manifested as increased RGS9-1 activity. However, such an increase of activity will saturate when the vesicle concentration exceeds that of RGS9-1. On the other hand, as the vesicle concentration approaches and exceeds that of RGS9-1, the probability of G<sub>αt</sub>-GTP being formed on a vesicle lacking RGS9-1 also increases. If G<sub>αt</sub>-GTP exchange between vesicles is very slow on the timescale of GTP hydrolysis, then at higher vesicle concentrations the apparent GAP activity must decline. Therefore, in order to determine the maximal enhancement of GAP activity by R9AP-containing vesicles, we performed a vesicle

titration, holding RGS9-1 concentration constant. RGS9-1 GAP activity ( $\Delta k_{\text{inact}}$ ) on rhodopsin-only or rhodopsin and R9AP vesicles were measured similarly as described earlier over a series of vesicle concentrations. Final concentrations in the reactions were vesicles: 9.0, 18, 36, 72, 144, 288, and 576 nM; rhodopsin: 0.38, 0.75, 1.5, 3.0, 6.0, 12.0, and 24.0  $\mu\text{M}$ ; R9AP: 0.12, 0.24, 0.48, 0.96, 1.9, 3.8, and 7.7  $\mu\text{M}$ ; GST-RGS9-1-G $\beta_5$ , 0.1  $\mu\text{M}$ , G $_t$ : 0.2  $\mu\text{M}$  (for vesicle concentrations from 9.0 to 36.0 nM) or 0.5  $\mu\text{M}$  (for vesicle concentrations from 72.0 to 576.0 nM). Enhancement on RGS9-1 GAP activity by R9AP membrane anchoring was defined as fold enhancement =  $\Delta k_{\text{inact}}$  (on rhodopsin and R9AP vesicles)/ $\Delta k_{\text{inact}}$  (on rhodopsin only vesicles) and was plotted as mean  $\pm$  standard deviation against vesicle concentration and R9AP concentration (on a log scale) (Fig. 3A).

*Mathematical Model for Data Analysis.* Because G $_t$  and RGS9-1-G $\beta_5$  should bind to rhodopsin- and R9AP-containing vesicles independently of one another, the apparent GAP activity should decline in a way predicted

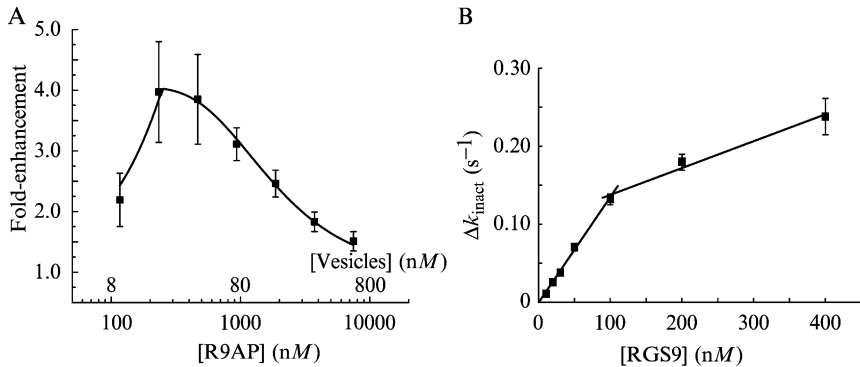


FIG. 3. Activation of GAP activity of RGS9-1 by reconstituted R9AP. (A) RGS9-1 GAP activity ( $\Delta k_{\text{inact}}$ ) toward transducin was measured on rhodopsin-only or rhodopsin and R9AP vesicles at different vesicle concentrations and compared to yield fold enhancement =  $\Delta k_{\text{inact}}$  (on rhodopsin and R9AP vesicles)/ $\Delta k_{\text{inact}}$  (on rhodopsin only vesicles), plotted as mean  $\pm$  standard deviation. The final GST-RGS9-1-G $\beta_5$  concentration was held constant at 0.1  $\mu\text{M}$ , and the G $_t$  concentration was 0.2  $\mu\text{M}$  for vesicle concentrations from 9.0 to 36.0 nM and 0.5  $\mu\text{M}$  for vesicle concentrations from 72.0 to 576.0 nM. The *continuous curve* was calculated using Eq (1), assuming a maximal enhancement of fourfold. (B) RGS9-1 GAP activity ( $\Delta k_{\text{inact}}$ ) on urea-washed ROS membranes was measured by single turnover assays as described in the text. Data were plotted as mean  $\pm$  standard deviation and fit to two linear functions (*straight lines*) with slopes of 1.36 and 0.34  $\mu\text{M}^{-1} \cdot \text{s}^{-1}$ . Reprinted, with permission, from Hu *et al.* (2003).

by Poisson statistics. Therefore, the probability of a vesicle having exactly  $x$  molecules of RGS9-1 when the average number of RGS9-1 molecules per vesicle is  $\mu$  can be calculated by the Poisson distribution [Eq. (1)]. Based on this assumption, together with the assumption that the dissociation constant  $K_d$  between RGS9-1 and R9AP on the vesicles was much lower than their concentrations used in the experiments and that each  $G\alpha_t$ ·GTP stays on the vesicle in which it was originally activated until its bound GTP is hydrolyzed, we were able to build the following mathematical model for the effect of R9AP on RGS9-1 GAP activity: Eq. (2) (Fig. 3A, smooth line).

$$P(x, \mu) = \mu^x e^{-\mu} / x! \quad (1)$$

$$E - 1 = (E_{\max} - 1) \times \left[ \frac{\text{(total concentration of accessible R9AP)}}{\text{(total concentration of RGS9)}} \times [1 - \exp(-\mu)], \right. \\ \left. \text{when accessible R9AP} \leq \text{RGS9, and by } E - 1 \right. \\ \left. = (E_{\max} - 1) \times [1 - \exp(-\mu)], \text{ when accessible R9AP} \geq \text{RGS9.} \right. \\ E, \text{ the expected fold enhancement (smooth line),} \\ E_{\max}, \text{ maximal fold enhancement of RGS9-1 activity} \quad (2)$$

### *Enhancement of RGS9-1 GAP Activity by Urea-Washed ROS Membranes*

It was reported previously that urea washing can expose endogenous binding sites for RGS9-1 on purified ROS, and binding of RGS9-1 to these sites enhances its activity. To compare our results on reconstituted vesicles to that on urea-washed ROS, we titrated different concentrations of recombinant RGS9-1 protein into urea-washed membranes held at a constant concentration and measured the GAP activity by single turnover assays.

#### *Buffers and Reagents*

Hypotonic buffer: 5 mM Tris-HCl, pH 7.4, 3 mM EDTA

4 M urea buffer: 4 M urea, 5 mM Tris-HCl, pH 7.4

6 M urea buffer: 6 M urea, 5 mM Tris-HCl, pH 7.4

GAPN buffer: 100 mM NaCl, 10 mM HEPES, pH 7.4, 2 mM MgCl<sub>2</sub>

1 mM DTT and solid PMSF are added to all these buffers before use

Proteins: GST-tagged RGS9-1·Gβ<sub>5</sub> and His<sub>6</sub>-PDEγ

Purified bovine ROS membranes (see earlier discussion)

*Procedures.* ROS membranes are washed sequentially with hypertonic buffer (twice), hypotonic buffer (twice), 4 M urea buffer (once), and GAPN buffer (twice). For each sequential washing step, ROS membranes are diluted, typically to  $\sim 10 \mu\text{M}$  rhodopsin, in the indicated buffer, homogenized extensively on ice using a glass/Teflon homogenizer, and centrifuged in a Ti-45 rotor (Beckman) at 44,000 rpm for 45 min. Washed membranes are resuspended in GAPN buffer and stored at  $-80^\circ$ .

For GAP assays, urea-washed ROS are incubated with purified  $G_t$ , His<sub>6</sub>-PDE $\gamma$ , and GST-RGS9-1 · G $\beta_5$  in GAPN buffer on ice for  $\sim 30$  min. GTP hydrolysis is initiated by adding [ $\gamma$ -<sup>32</sup>P]GTP, and the GTP hydrolysis rate constant is determined using the single turnover method described earlier. Typical final concentrations of proteins are rhodopsin, 72  $\mu\text{M}$ ;  $G_t$ , 0.5  $\mu\text{M}$ ; His<sub>6</sub>-PDE $\gamma$ , 0.2  $\mu\text{M}$ , and GST-RGS9-1 · G $\beta_5$ , 10, 20, 30, 50, 100, 200, and 400 nM. RGS9-1 GAP activity ( $\Delta k_{\text{inact}}$ ) is plotted against its concentration as mean  $\pm$  standard deviation and is fitted with straight lines (Fig. 3B). GAP assays using 6 M urea buffer-washed ROS yields similar results to those using 4 M urea buffer-washed membranes, except that there is a slightly decreased  $k_{\text{cat}}/K_m$  value of RGS9-1 · G $\beta_5$  on 6 M urea-treated membranes.

## Acknowledgments

This work was supported by National Eye Institute Grant R01-EY11900, the Robert A. Welch Foundation, and the National Center for Macromolecular Imaging, P41-RR02250.

## References

- Chen, C. K., Burns, M. E., He, W., Wensel, T. G., Baylor, D. A., and Simon, M. I. (2000). Slowed recovery of rod photoresponse in mice lacking the GTPase accelerating protein RGS9-1. *Nature* **403**, 557–560.
- Chen, P. S., Toribara, T. Y., and Warner, H. (1956). Microdetermination of phosphorous. *Anal. Chem.* **28**, 1756–1758.
- Cowan, C. W., Wensel, T. G., and Arshavsky, V. Y. (2000). Enzymology of GTPase acceleration in phototransduction. *Methods Enzymol.* **315**, 524–538.
- Cowan, C. W., He, W., and Wensel, T. G. (2001). RGS proteins: Lessons from the RGS9 subfamily. *Prog. Nucleic Acid Res. Mol. Biol.* **65**, 341–359.
- Cowan, C. W., Fariss, R. N., Sokal, I., Palczewski, K., and Wensel, T. G. (1998). High expression levels in cones of RGS9, the predominant GTPase accelerating protein of rods. *Proc. Natl. Acad. Sci. USA* **95**, 5351–5356.
- Daemen, F. J. M. (1973). Vertebrate rod outer segment membranes. *Biochim. Biophys. Acta* **300**, 255–288.
- Gray, G. D., Mickelson, M. M., and Crim, J. A. (1969). The demonstration of two gamma-globulin subclasses in the goat. *Immunochemistry* **6**, 641–644.
- Harlow, E., and Lane, D. (1988). “Antibodies: A Laboratory Manual.” Cold Spring Harbor Laboratories, Cold Spring Harbor, NY.

- He, W., Cowan, C. W., and Wensel, T. G. (1998). RGS9, a GTPase accelerator for phototransduction. *Neuron* **20**, 95–102.
- He, W., Lu, L., Zhang, X., El-Hodiri, H. M., Chen, C. K., Slep, K. C., Simon, M. I., Jamrich, M., and Wensel, T. G. (2000). Modules in the photoreceptor RGS9-1.Gbeta 5L GTPase-accelerating protein complex control effector coupling, GTPase acceleration, protein folding, and stability. *J. Biol. Chem.* **275**, 37093–37100.
- He, W., and Wensel, T. G. (2002). RGS function in visual signal transduction. *Methods Enzymol.* **344**, 724–740.
- Hu, G., Jang, G. F., Cowan, C. W., Wensel, T. G., and Palczewski, K. (2001). Phosphorylation of RGS9-1 by an endogenous protein kinase in rod outer segments. *J. Biol. Chem.* **276**, 22287–22295.
- Hu, G., and Wensel, T.G. (2002). R9AP, a membrane anchor for the photoreceptor GTPase accelerating protein, RGS9-1. *Proc. Natl. Acad. Sci. USA* **99**, 9755–9760.
- Hu, G., Zhang, Z., and Wensel, T. G. (2003). Activation of RGS9-1 GTPase acceleration by its membrane anchor, R9AP. *J. Biol. Chem.* **278**, 14550–14554.
- Ibrahimi, I. M., Eder, J., Prager, E. M., Wilson, A. C., and Arnon, R. (1980). The effect of a single amino acid substitution on the antigenic specificity of the loop region of lysozyme. *Mol. Immunol.* **17**, 37–46.
- Lishko, P. V., Martemyanov, K. V., Hopp, J. A., and Arshavsky, V. Y. (2002). Specific binding of RGS9-Gbeta 5L to protein anchor in photoreceptor membranes greatly enhances its catalytic activity. *J. Biol. Chem.* **276**, 24376–24381.
- Lyubarsky, A. L., Naarendorp, F., Zhang, X., Wensel, T., Simon, M. I., and Pugh, E. N., Jr. (2001). RGS9-1 is required for normal inactivation of mouse cone phototransduction. *Mol. Vis.* **7**, 71–78.
- Lyubarsky, A. L., and Pugh, E. N., Jr. (1996). Recovery phase of the murine rod photoresponse reconstructed from electroretinographic recordings. *J. Neurosci.* **16**, 563–571.
- Makino, E. R., Handy, J. W., Li, T., and Arshavsky, V. Y. (1999). The GTPase activating factor for transducin in rod photoreceptors is the complex between RGS9 and type 5 G protein beta subunit. *Proc. Natl. Acad. Sci. USA* **96**, 1947–1952.
- Martemyanov, K. A., and Arshavsky, V. Y. (2002). Noncatalytic domains of RGS9-1. Gbeta 5L play a decisive role in establishing its substrate specificity. *J. Biol. Chem.* **277**, 32843–32848.
- Papermaster, D. S. (1982). Preparation of retinal rod outer segments. *Methods Enzymol.* **81**, 48–52.
- Papermaster, D. S., and Dreyer, W. J. (1974). Rhodopsin content in the outer segment membranes of bovine and frog retinal rods. *Biochemistry* **13**, 2438–2444.
- Parmar, M. M., Edwards, K., and Madden, T. D. (1999). Incorporation of bacterial membrane proteins into liposomes: Factors influencing protein reconstitution. *Biochim. Biophys. Acta* **1421**, 77–90.
- Pugh, E. N., Jr., and Lamb, T. D. (2000). “Phototransduction in Vertebrate Rods and Cones: Molecular Mechanisms of Amplification, Recovery and Light Adaptation.” Elsevier, New York.
- Quick, M., and Wright, E. M. (2002). Employing *Escherichia coli* to functionally express, purify, and characterize a human transporter. *Proc. Natl. Acad. Sci. USA* **99**, 8597–8601.
- Sagoo, M. S., and Lagnado, L. (1997). G-protein deactivation is rate-limiting for shut-off of the phototransduction cascade. *Nature* **389**, 392–395.
- Slep, K. C., Kercher, M. A., He, W., Cowan, C. W., Wensel, T. G., and Sigler, P. B. (2001). Structural determinants for regulation of phosphodiesterase by a G protein at 2.0 Å. *Nature* **409**, 1071–1077.

- Sokal, I., Hu, G., Liang, Y., Mao, M., Wensel, T. G., and Palczewski, K. (2002). Identification of protein kinase C isozymes responsible for the phosphorylation of photoreceptor-specific RGS9-1 at Ser475. *J. Biol. Chem.* **278**, 8316–8325.
- Struthers, M., Yu, H., and Oprian, D. D. (2000). G protein-coupled receptor activation: Analysis of a highly constrained, “straitjacketed” rhodopsin. *Biochemistry* **39**, 7938–7942.
- Zhang, X., Wensel, T. G., and Kraft, T. W. (2003). GTPase regulators and photoresponses in cones of the eastern chipmunk. *J. Neurosci.* **23**, 1287–1297.

## [13] Kinetic Approaches to Study the Function of RGS9 Isoforms

By KIRILL A. MARTEMYANOV and VADIM Y. ARSHAVSKY

### Abstract

The experimental strategies developed in kinetic studies of interactions between RGS9 isoforms with G proteins of the G<sub>i</sub> subfamily provide a useful framework for conducting similar studies with essentially any regulator of G-protein signaling (RGS) protein – G-protein pair. This article describes two major kinetic approaches used in the studies of RGS9 isoforms: single turnover and multiple turnover GTPase assays. We also describe pull-down assays as a method complementary to the kinetic assays. The discussion of the strengths and limitations of each individual assay emphasizes the importance of combining multiple experimental approaches in order to obtain comprehensive and internally consistent information regarding the mechanisms of RGS protein action.

### Introduction

Regulator of G-protein signaling (RGS) proteins regulate the duration of G-protein signaling by stimulating GTP hydrolysis on the G-protein  $\alpha$  subunits ( $G\alpha$ ), thus determining the lifetime of G proteins in their active states. For this reason, RGS proteins can be considered enzymes that catalyze the conversion of the active state of  $G\alpha$ ,  $G\alpha \cdot GTP$ , to its inactive state,  $G\alpha \cdot GDP$ . In all RGS proteins, this catalysis is performed by the  $\sim 120$  amino acid-long RGS homology domain. RGS homology domains of different RGS proteins have different catalytic efficiencies and different spectra of G-protein specificity. Furthermore, most RGS proteins are equipped with additional noncatalytic domains that can drastically modify the catalytic properties of RGS homology domains or couple RGS proteins to their regulators. This versatility in modulating the catalytic activity of